JSHC
Japan Society of
Histochemistry and Cytochemistry
Established 1959

Acta Histochem. Cytochem. 49 (6): 159–169, 2016
doi: 10.1267/ahc.16017

Morphological Changes of Myoepithelial Cells in the Rat Submandibular Gland Following the Application of Surgical Stimuli

Yoshihiro Kawabe[1,2], Kenich Mizobe[1,2], Yasuhiko Bando[1], Koji Sakiyama[1], Fuyoko Taira[1,3], Akito Tomomura[4], Hisao Araki[2] and Osamu Amano[1]

[1]Division of Anatomy, Meikai University School of Dentistry, Sakado, Saitama, Japan, [2]Division of Oral Rehabilitation, Meikai University School of Dentistry, [3]Division of Oral and Maxillofacial Surgery II, Meikai University School of Dentistry and [4]Division of Biochemistry, Meikai University School of Dentistry

Received May 11, 2016; accepted August 23, 2016; published online December 23, 2016

Myoepithelial cells (MECs) exist on the basal surface of acini in major exocrine glands, include myofilaments and various constructive proteins, and share characteristics with smooth muscle and epithelial cells. MECs project several ramified processes to invest acini, and possibly contract to compress acini to support the secretion by the glandular cells. However, the functional roles of MECs in salivary secretion are still unclear. We investigated morphological changes in immunostained MECs using the anti-α-smooth muscle actin (αSMA) antibody in operated or non-operated contralateral (NC) submandibular glands after partial or total resection. Furthermore, we investigated and discuss other salivary glands of rats. MECs in the parotid, sublingual and submandibular gland of adult rats exhibited different shapes and localizations. After surgery, in both operated and NC glands, the number of MECs and αSMA-immunopositive areas increased significantly. Three-dimensional analysis using a confocal laser-scanning microscope revealed that substantial and significant enhancement became evident in the number, length, and thickness of MEC-processes covering acini of the operated and NC submandibular glands. The preset findings indicate that MECs alter the morphology of their processes in operated and NC glands after surgery of the partial or total resection. It is suggested that MECs promote salivary secretion using elongated, thickened, and more ramified processes.

Key words: myoepithelial cell, α-smooth muscle actin, immunohistochemistry, submandibular gland, rat

I. Introduction

Myoepithelial cells (MECs) are multipolar stellate cells possessing many long processes intervening between the basement membrane and basal surface of acinar cells in major exocrine glands [49]. MECs were discovered and termed as "stellate cells (*sternförmige Zellen*)" in cat salivary glands and had also been termed "basket cells (*Korbzellen*)"; however, they are now generally referred to as MECs after Renaut proposed this term in 1897 [36]. Electron microscopic analyses showed that the MEC cytoplasm is filled with thin myofilaments arranged in parallel and immunoreactive for α-smooth muscle actin (αSMA) [36, 43]. MECs contain various contractile proteins, such as myosin, calponin, and caldesmon, in addition to αSMA [26, 30, 36]. MECs originate from glandular epithelia, the same as acinar cells [8]. MECs express epithelial markers, including various types of cytokeratins [30], but lack mesenchymal cell markers, such as vimentin [30]. Therefore, MECs share similar characteristics with smooth muscle and epithelial cells.

Three-dimensional (3D) analysis of MECs by scan-

Correspondence to: Osamu Amano, Division of Anatomy, Meikai University School of Dentistry, 1–1 Keyakidai, Sakado, Saitama 350–0283, Japan. E-mail: oamano@dent.meikai.ac.jp

ning electron microscopy showed that MECs project several branched processes from the cell body containing the nucleus [6]. Based on these histological and histochemical characteristics, MECs are speculated to assist in the release of secretory components by covering acini with their contractile processes [12, 28, 35]; however, they are absent in typical exocrine tissue, the pancreas in humans and other mammals [20, 14, 36] and rodent parotid acini [36]. Thus, MECs are not regarded as essential for exocrine secretion, and their functional significance still remains unclear [35].

MECs are present in all salivary glands in humans [36], with neoplastic transformation occasionally occurring and inducing various salivary gland tumors [10, 28, 35, 36]. Therefore, it is assumed that MECs not only contract for secretion, but also dynamically alter their shape in response to changes in conditions and stimulations to correspond to various functional states. The morphology of MECs in the mammary gland markedly changes with pregnancy-induced differentiation and milk secretion after delivery, and becomes irregular with complex processes during the lactation period [32, 33, 47].

When salivary glands are damaged by tumors, inflammation, or calculi, cells of the normal tissue proliferate and/or become hypertrophic, generally described as 'compensate hypertrophy' [4, 34, 38, 42]. When surgical resection is performed to remove damaged tissue, repair and regeneration occur rapidly in the rest of the normal tissues on the surgical side of bilateral organs/tissues; in addition, hypertrophic reactions may occur in normal tissue on the non-surgical contralateral (NC) side to compensate [38]. Compensatory hypertrophy has been reported in the liver following partial resection, and in the lung after unilateral excision [48]. The quantitative compensation of secretory function by proliferation of acinar cells and MECs during regeneration has also been reported [15, 40, 41]. Our recent study showed that salivary gland resection induced acinar cell differentiation from the intercalated duct in the residual tissue of the operated side, as well as the NC side in adult rats [25]. An increased salivary secretion from the residual acini is necessary to complement decreased glandular tissue resulting from surgery resection.

Neurological [23, 31, 39], hormonal [21, 24, 44, 45], and drug [17, 37, 46] stimulations enhance salivary secretion via their receptors or ion channels [7]. However, the mechanisms by which MECs regulate salivary secretion have not yet been established.

In the present study, we performed immunohistochemical analysis using an anti-αSMA antibody and laser microscopic 3D analysis as follows: 1) the distribution and morphology of MECs in the rat major salivary glands; 2) postnatal growth and aging of MECs in the rat submandibular gland; and 3) morphological changes in MECs after unilateral partial or total resection, on both the operated and NC sides.

II. Materials and Methods

Experimental animals and surgery

Twenty-one male Wistar rats were used as the untreated group: 3 animals each at 3, 8, 9, 10, 12, 16, and 48 weeks old (W). Surgery was performed on 18 8W male rats weighing approximately 200 g: 12 and 6 animals in the partial resection and total resection groups, respectively. Animals were maintained according to the Meikai University guidelines for experiments. They were fed pellets and given free access to drinking water during the experimental period. This study was performed after approval by the Animal Ethics Committee of Meikai University School of Dentistry (A1316).

Surgery on the submandibular gland was performed using the procedure reported by Mizobe *et al.* [25]. Under general anesthesia with an intraperitoneal injection of 1 mL/kg pentobarbital sodium (Somnopentyl, Kyoritsu Seiyaku, Tokyo, Japan), the rat was placed in a supine position, an incision was made in the right submandibular skin, and connective tissue was dissected while avoiding damage to the surrounding tissue, including nerves and blood vessels.

Partial resection of the right submandibular gland (PX)

After skin dissection, connective tissue around the right submandibular gland including the capsule was carefully dissected as described above, and the body of the gland was exposed. The central region of the body of the submandibular gland was ligated with silk thread, avoiding inclusion of the sublingual gland, the distal portion far from the submandibular duct was resected, and the wound was closed using sutures. Animals were fixed by perfusion 1, 2, 4, or 8 W after partial resection, and the operated (right) and NC (left) submandibular glands were excised.

Total resection of the right submandibular and sublingual glands (TX)

The right submandibular gland was exposed, as described above. The right submandibular and sublingual gland ducts were ligated with silk thread, the right submandibular and sublingual glands covered with the same capsule were excised *en bloc*, and the wound was closed using sutures. Animals were fixed by perfusion 1 or 2 weeks after total resection, and the submandibular gland on NC side (left) was excised.

Fixation and general staining

Under general anesthesia with an intraperitoneal injection of 1 mL/kg pentobarbital sodium (Somnopentyl), the animal was perfused with saline through the left ventricle to remove blood, followed by perfusion fixation with 4% paraformaldehyde/0.1 M phosphate buffer (pH 7.4). The residual submandibular gland was excised from the operated rats, and the parotid and sublingual glands, in addition to the submandibular gland, and the pancreas were excised

from normal rats. Specimens were immersed in the same fixative overnight, and then in 30% sucrose/0.1 M phosphate buffer (pH 7.4) for 24 hr or longer. Six- and 20-μm-thick frozen sections were then prepared. Some of the 6-μm-thick sections were stained with hematoxylin-eosin (H-E) according to the standard method and observed under a light microscope.

Immunohistochemistry

Immunostaining for light microscopy

Six-μm-thick frozen sections were used for conventional immunohistochemical staining. Sections were dried at room temperature (RT) and immersed in phosphate-buffered saline (0.01 M phosphate buffer, 0.15 M NaCl, pH 7.4, PBS) containing 0.3% Triton-X-100 for 30 min. After washing with PBS, the sections were treated with 0.1% H_2O_2/methanol for 10 min to inhibit endogenous peroxidase activity. After washing with distilled water and PBS, a mouse anti-rat αSMA monoclonal antibody (ACTA2, 1:200, Abnova, Taipei, Taiwan) was applied at RT overnight. After washing with PBS, the sections were reacted with biotin-conjugated secondary antibody and then horseradish peroxidase (HRP)-labeled streptavidin solution at RT for 60 min each using LSAB II System-HRP for use on rat specimens (Dako, Carpentaria, CA, USA). Visualization was made using 0.01% H_2O_2-containing 3.3-diaminobenzidine tetrahydrochloride (DAB, Dojindo, Kumamoto, Japan), and sections were dehydrated and penetrated. For the negative control, immunostaining procedures were made with PBS instead of the primary antibody, and confirmed the absence of nonspecific immunoreactions.

Western blotting

Normal 10W rat submandibular glands (n=3) and NC side of PX-2W submandibular glands (n=3) were solubilized (1/10 weight/volume) in sampling buffer (10% glycerol, 60 mM Tris pH 6.8, 2% SDS, 0.01% bromophenol blue, 2% beta-mercaptoethanol) using Dounce homogenizer. Samples were separated by SDS-PAGE, transferred onto Immobilon-P PVDF membrane (Millipore), and then immunoblotted with antibodies against mouse anti-rat αSMA (ACTA2, 1:200) or rabbit anti-human glyceraldehyde 3-phosphate dehydrogenase (GAPDH, 1:1000; Trevigen, Gaithersburg, MD). The blot was incubated with horseradish peroxidase-conjugated secondary antibodies (Cell signaling Technology Japan, Tokyo, Japan), and chemiluminescence was detected with Clarity Western ECL Substrate (Bio-Rad, Hercules, CA, USA).

Immunostaining for laser microscopy

Twenty-μm-thick sections were used for confocal laser scanning microscopy (CLSM) to analyze 3D morphology. After drying at RT, sections were immersed in 0.3% Triton-X-100/PBS (pH 7.4) for 60 min, washed with PBS, and treated with 10% normal goat serum (Nichirei) at RT for 30 min. After washing with PBS, the sections were reacted with a mouse anti-rat αSMA (ACTA2) monoclonal antibody (1:200, Abnova) at RT overnight. After washing with PBS, the sections were reacted with a Cy3-conjugated donkey anti-mouse IgG polyclonal antibody (1:500, Merck Millipore, Billerica, MA, USA), at RT for 60 min. After washing with PBS, the sections were mounted using Fluoroshield Mounting Medium (Immuno BioScience, Mukilteo, WA, USA), and observed under a CLSM (LSM-510, Carl Zeiss, Jene, Germany). For 3D analysis, the sample was continuously imaged at 1-μm-thick intervals using Z-stacks, according to the method of Bando *et al.* [5], and a 3D image was reconstructed on a computer.

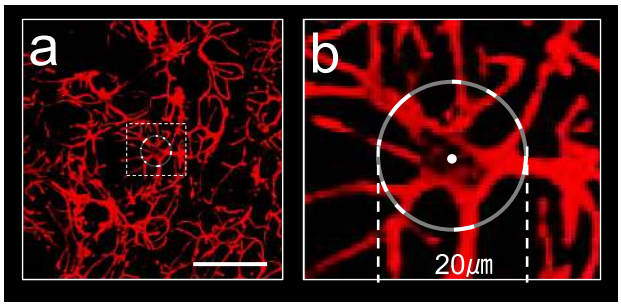

Fig. 1. Lower (**a**) and higher (**b**; dotted square in **a**) images of confocal laser-scanning microscopy (CLSM) demonstrating the thickness of the myoepithelial cell processes of the rat submandibular gland immunostained for αSMA. For the thickness of a myoepithelial cell process, the length of the portion of the circle 20 μm in diameter with its center at the center of the nucleus intersecting with the process was measured. Bar=50 μm.

Morphometry and statistical analysis

After immunohistochemical staining, 10 visual fields, each 332 μm×415 μm in area, were randomly selected from sections in each experimental condition. In the present study, a MEC with a clearly observable cell body containing a nucleus was counted as a cell. And the number of MECs positive for an immunoreaction with αSMA and the area occupied by these cells were measured. The area was measured using Image J (The Research Services Branch, National Institute of Mental Health, Bethesda, MD, USA). After reconstructing the laser microscopic 3D, 10 MECs were randomly selected in each experimental group, and the number and thickness of the processes were measured. Processes branching from the cell body were regarded as 'primary processes', the tips of the processes after repeated branching were regarded as 'terminal processes', and these were counted. The thickness of processes was measured, as shown in Figure 1: A circle with a 20 μm diameter centering on the nucleus of the MEC was lined up, and the width of a process crossing over the circle was measured. The value calculated by dividing the sum of the process widths by the number of processes measured was regarded as the process thickness (Fig. 1a, b).

In western blot analysis the protein content of αSMA

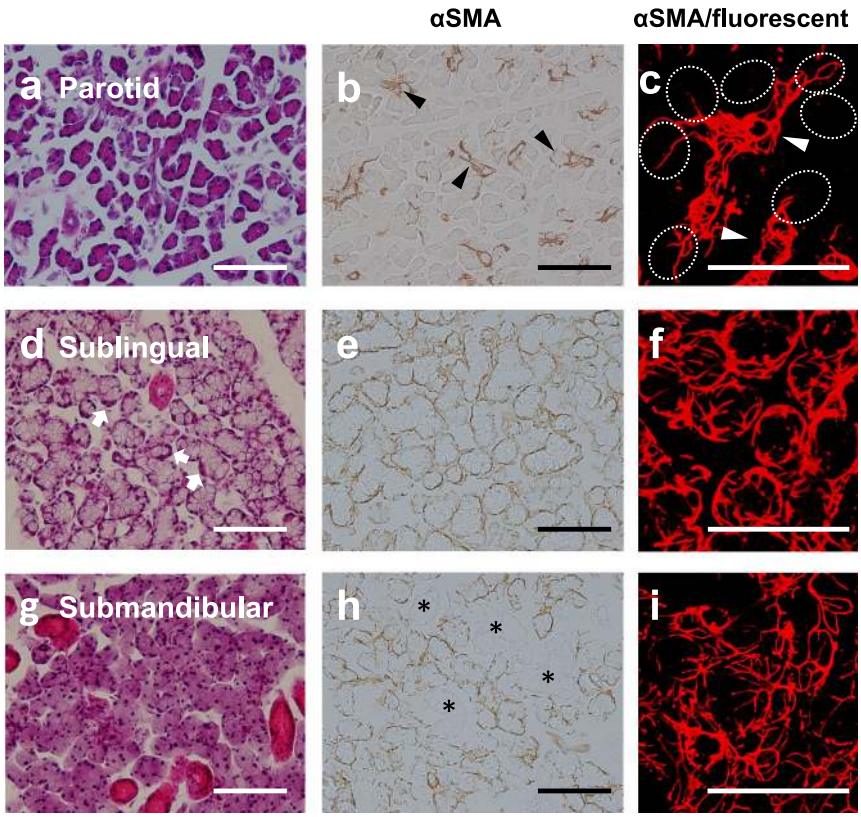

Fig. 2. Microphotographs of H-E staining (**a, d, g**), conventional (**b, e, h**), and higher magnified CLSM immunohistochemistry (**c, f, i**) stained for αSMA of parotid (**a–c**), sublingual (**d–f**), and submandibular (**g–i**) glands of adult rats. The parotid gland includes developed serous acini, as well as intercalated and striated ducts (**a**). αSMA-positive myoepithelial cells are rarely on the acini (dotted circles in **c**), but present along the intercalated duct (arrowheads in **b, c**). The sublingual gland consists of mixed acini accompanying the serous demilune (arrows in **d**). Sublingual myoepithelial cells thickly covered mixed acini (**e**), and their processes are relatively shorter and simpler (**f**) than those of the submandibular gland (**i**). The submandibular gland consists of developed serous acini, as well as intercalated, granular, and striated ducts, and lacks mucous cells (**g**). Submandibular myoepithelial cells cover both acini and intercalated ducts (**h**), and their processes are relatively longer and more complicated (**i**) than those of the sublingual gland (**f**). Granular and striated ducts (*) lack myoepithelial cells. Bar=100 μm.

and GAPDH were quantified using ImageJ, and expression of αSMA in the normal gland and PX-2W NC side) were compared by the ratio of αSMA to GAPDH.

The number and area of MECs, the number and thickness of processes determined by 3D analysis and αSMA/GAPDH ratio determined by Western blotting were presented as mean±SD in graphs, and compared between an experimental group (n=3, respectively) and a control group (n=3, respectively) using the Mann-Whitney U-test, with $p<0.05$ or $p<0.01$ being defined as significant.

III. Results

MECs in major salivary glands

Since the properties and chemical composition of saliva vary among the major salivary glands in the rat [3, 16], MECs in the normal salivary glands were observed and analyzed in 8W rats in order to determine the relationship between saliva and MECs.

Parotid gland

In the normal parotid gland at 8W, acinar cells were comprised homogenously of serous cells, and intercalated and striated ducts had developed (Fig 2a). Immunohistochemistry with αSMA showed that MECs were mainly localized in the intercalated ducts and rarely in acini (Fig. 2b). Laser microscopic observations revealed that the processes of MECs extended along the distribution of the intercalated ducts (Fig. 2c).

Sublingual gland

The normal sublingual gland in 8W rats is a mixed gland consisting of central-located mucous cells and peripheral serous demilune in acini, similar to human sublingual glands [3] (Fig. 2d). By conventional immunohistochemistry, MECs positive for αSMA were found to be relatively thick and covered the entirety of the basal surface of acini (Fig. 2e). The laser microscopic 3D morphology analysis showed that 2 or 3 MECs were present for one acinus, their processes were thick and short, and branching

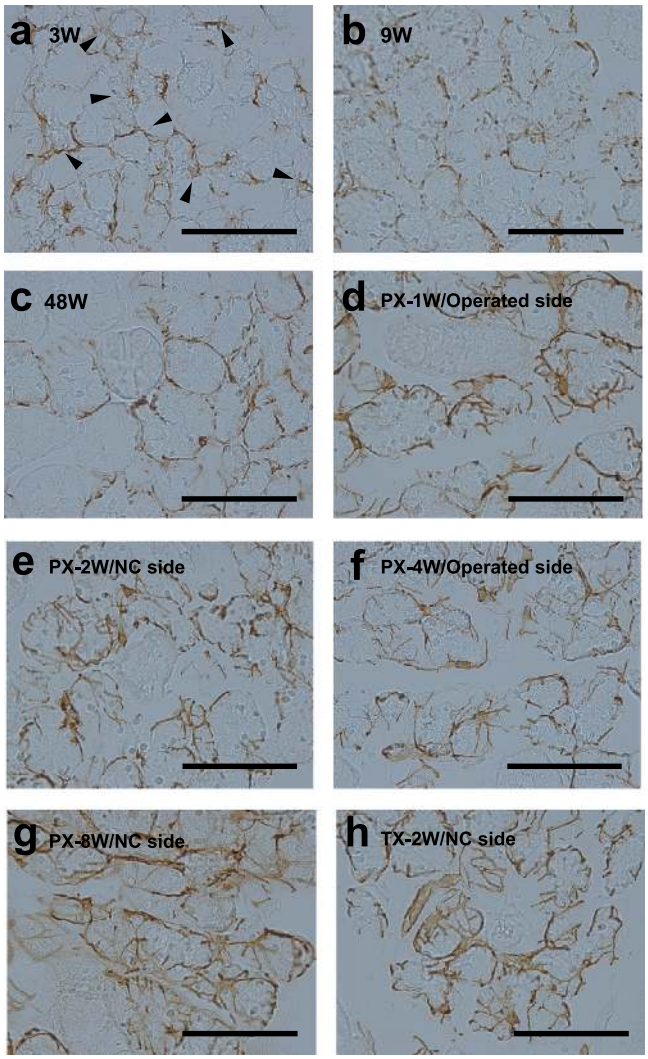

Fig. 3. Photomicrographs showing conventional immunohistochemistry for αSMA in normal MECs in suckling rats were mainly present in the intercalated ducts (arrowheads in **a**) (**a–c**) and post-operated (**d–h**) submandibular glands of rats. Note that the shape of the myoepithelial cells and their processes in post-operated rats was more complicated than those of normal rats. Bar=100 μm.

was relatively simple rather those of the submandibular gland described below (Fig. 2f).

Submandibular gland

The human submandibular gland is a mixed gland in which acini accompanied by serous demilunes are present; whereas in 8W rat submandibular glands, acini were comprised of only serous cells [3]. Intercalated and striated ducts were prominent, in addition to granular ducts secreting various types of growth factors [3] (Fig. 2g). Immunohistochemical staining revealed that αSMA-positive MECs were present in the acini and intercalated ducts, but absent in the other ducts, including the granular and striated ducts. One or two MECs thinly covered one acinus, whereas no MEC bodies, including the nucleus or branching processes, were observed using this method (Fig. 2h). CLSM observations showed that MECs in acini projected several primary processes, branching 2 or 3 times. In the intercalated duct, MECs extend their processes longitudinally (Fig. 2i).

Pancreas

The rat pancreas is also comprised of both an exocrine portion and an endocrine portion (the islets of Langerhans) [13]. No αSMA-immunoreactivity was observed in the exocrine portion showing pure serous glands, excluding smooth muscle cells around the blood vessels (data not shown), confirming that MECs were absent in the rat pancreas, similar to that in humans [36].

The distribution and morphology of MECs in the normal rat salivary glands described above were mostly consistent with previous findings obtained using other histological methods, including electron microscopy [6, 27, 36, 43].

Aging- and surgery-induced changes in MECs in conventional immunostaining

Rat MECs in the suckling period and changes with aging

In normal submandibular glands of 3W rats, MECs were rarely around immature acini comprised of terminal tubules [36], and were mainly present in the intercalated ducts (Fig. 3a). In the normal submandibular gland at 48W, αSMA-positive MECs thinly surrounded acini, as observed at 9W (Fig. 3b, c).

Changes in MEC morphology after surgical resection

One week after PX (PX-1W) and PX-4W on the operated side, and PX-2W, PX-8W, and TX-2W on the NC side, abundant αSMA-positive MECs were found to extend processes covering acini, and many MEC bodies containing the nucleus were observed at the acini and intercalated ducts (Fig. 3d–h).

These changes were common to the operated and NC sides after PX, and the NC side after TX, throughout the experimental period.

Aging- and surgery-induced changes in the number of MECs

The number of MECs per unit area (332×415 μm^2) was measured (Fig. 4a). In the untreated normal submandibular gland, the number of MECs was significantly higher at 3W than at 9W. After 9W, the mean was 12.75–15.75, showing no marked change, and no significant change was noted even at 48W.

On the operated side of PX rats, the number of MECs at PX-1W was significantly higher than those in untreated normal rats of the same age (9W). The number at PX-2W, PX-4W, and PX-8W increased with time. A significant difference was noted over that in untreated rats of the same age throughout the experimental period (9–16W). Specifically, the number of MECs at PX-4W was approximately 5-fold higher than that in untreated rats of the same age (12W).

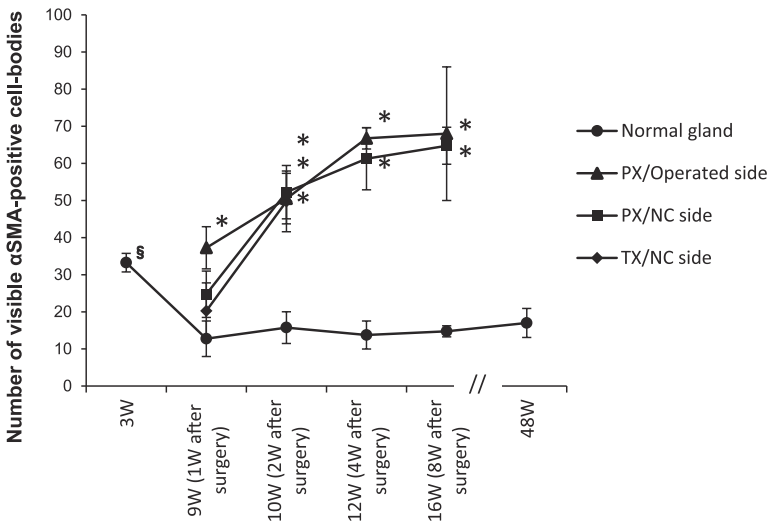

Fig. 4. Graph showing the chronological changes in the number of visible cell bodies of αSMA-immunopositive myoepithelium. Cell bodies including the nucleus in an area of 332×415 μm^2. *: significant $p<0.05$ compared with normal glands of the same age. §: significant $p<0.05$ compared with 9W normal glands.

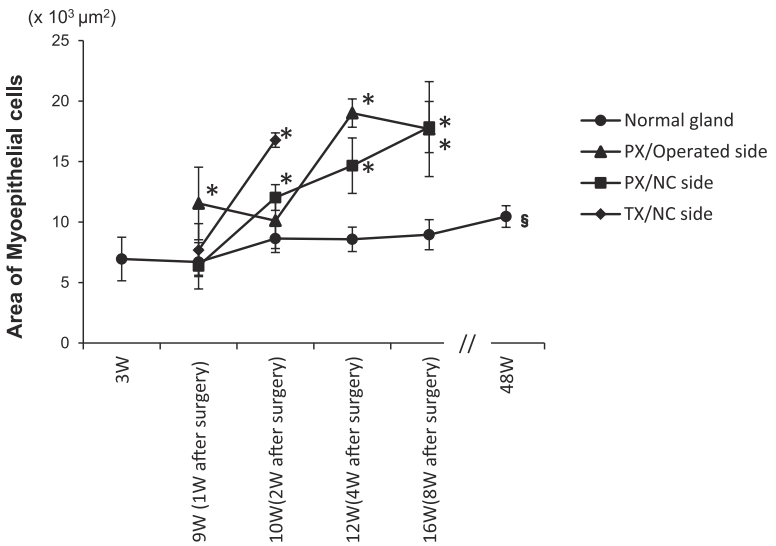

Fig. 5. Graph showing the chronological changes of αSMA-immunostained areas in 332×415 μm^2 of normal and post-operative submandibular glands of rats. *: significant $p<0.05$ compared with normal glands of the same age. §: significant $p<0.05$ compared with 9W normal glands.

On the NC side of PX rats, the number at PX-1W was slightly higher than in untreated rats of the same age (9W). However, the number of MECs at PX-2W was significantly higher than in untreated rats of the same age (10W), and continuously increased thereafter.

On the NC side of TX rats, the number slightly increased at TX-1W compared to untreated rats of the same age (9W), but was significantly higher, by approximately 3-fold, at TX-2W than in untreated rats of the same age (10W).

Changes in MEC size

The area immunoreactive for αSMA per unit (332× 415 μm^2) was measured as an index of MEC size (Fig. 5). The mean rate in the normal submandibular gland in untreated rats was approximately 6%, and slightly increased from 3W to 16W. This significantly increased to 7.6% at 48W. The mean rate at all time points was significantly higher on the operated side of PX (7.3–13.8%) than in untreated rats of the same age (4.8–6.4%).

On the NC side in PX rats, no significant differences were observed in the mean rate at PX-1W (4.6%) and that in untreated rats at the same age (9W) (4.8%); however, the mean rate at PX-2W (8.7%) was significantly higher than that in untreated rats of the same age (10W) (6.3%), and continued to increase with time (10.6–12.9%). On the NC side in TX rats, the rate slightly increased at TX-1W (5.5%) and significantly increased at TX-2W (12.2%).

In Western blot analysis, protein samples prepared from submandibular glands of the NC side of PX-2W

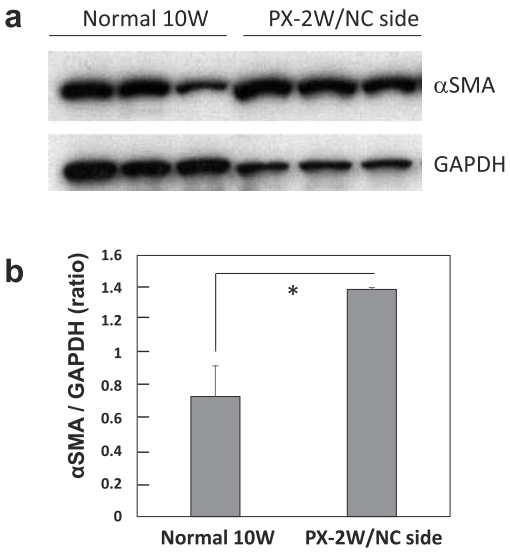

Fig. 6. αSMA content in the normal and post-operated submandibular glands of rats. Western blot analysis of αSMA and GAPDH (**a**). αSMA were quantified as the ratio of αSMA to GAPDH (**b**). The results represent means±SD for 3 glands. *: significant $p<0.05$.

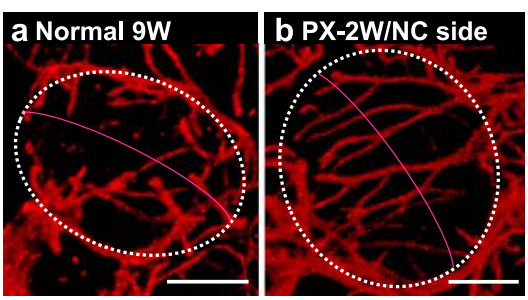

Fig. 7. CLSM 3-dimensional images of αSMA-immunostained myoepithelial cells of normal (**a**) and post-operated (**b**) submandibular glands of rats. Note that myoepithelial processes of the post-operated submandibular glands were elongated and were beyond the equator of the acinus. Bar=20 μm.

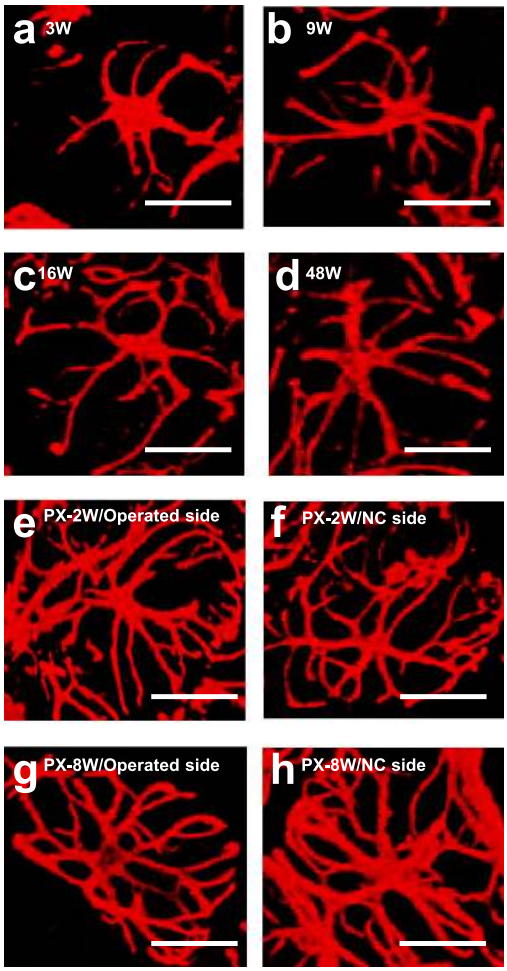

Fig. 8. CLSM-three-dimensional images of αSMA-immunostained myoepithelial cells of normal (**a–c**) and post-operated (**d–h**) submandibular glands of rats. Due to postnatal growth and post-operative changes, myoepithelial processes elongated and their ramification became intense. Bar=20 μm.

(10W) showed higher density (approximately 2-fold) of αSMA-immunoreactivity than those from normal 10W (Fig. 6a, b).

Morphological changes in individual MECs on CLSM

Since no marked difference was noted in changes after surgery between PX and TX in the conventional immunostaining, the morphology of individual MECs was analyzed in normal and PX rats.

Length of processes

Images of MECs in the lateral view of acini are shown in Figure 7. In the 9W normal rats, MEC processes were relatively short, and those of MECs located at the opposite poles of an acinus were not in contact or overlapping each other. When the spherical acinus is compared to the earth, no process tips crossed over the equator (Fig. 7a). In contrast, on the NC side at PX-2W, many processes passed over the equator, branched complicatedly, and crossed processes extended from the opposite pole (Fig. 7b). These changes were observed on both the operated and NC sides of the PX rats at all time points.

Number of processes

Thick processes that directly extended from the cell body as primary processes and the tips of processes after repeated branching as terminal processes were measured. The typical MECs of each experimental group are shown in Figure 8, and time-course changes in the number of processes are shown in Figure 9. In the 3W normal group, the number of primary processes (5.8) was not significantly different from that at any age; however, the number of terminal processes (20.4) was significantly fewer than those at the other ages (Fig. 8a). The numbers of primary (5.0–5.5) and terminal (25.5–26.3) processes did not markedly change from 9 to 16W in the normal group (Fig. 8b, c), but the number of terminal processes (29.3) slightly increased

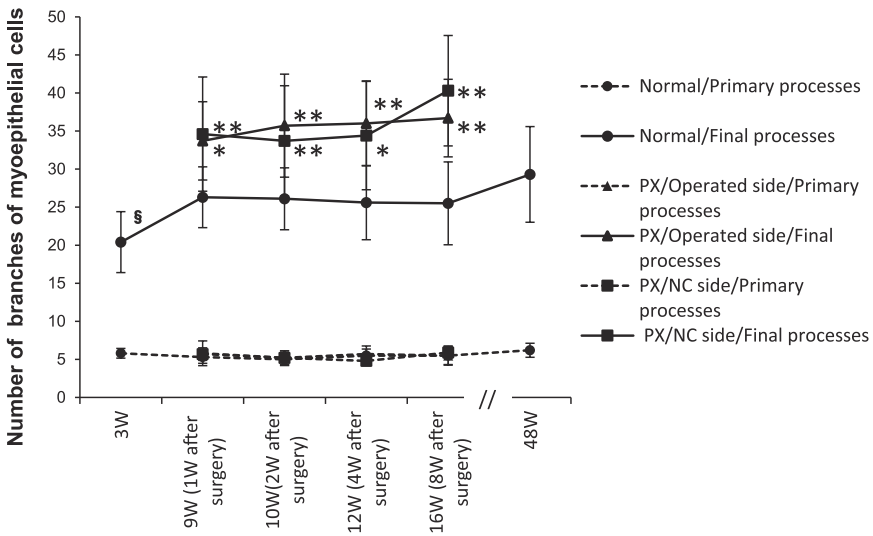

Fig. 9. Graph showing chronological changes in the number of primary and terminal processes of myoepithelial cells of normal and post-operated submandibular glands of rats. *: significant $p<0.05$ compared with normal glands of the same age. **: significant $p<0.01$ compared with normal glands of the same age. §: significant $p<0.05$ compared with 9W normal glands.

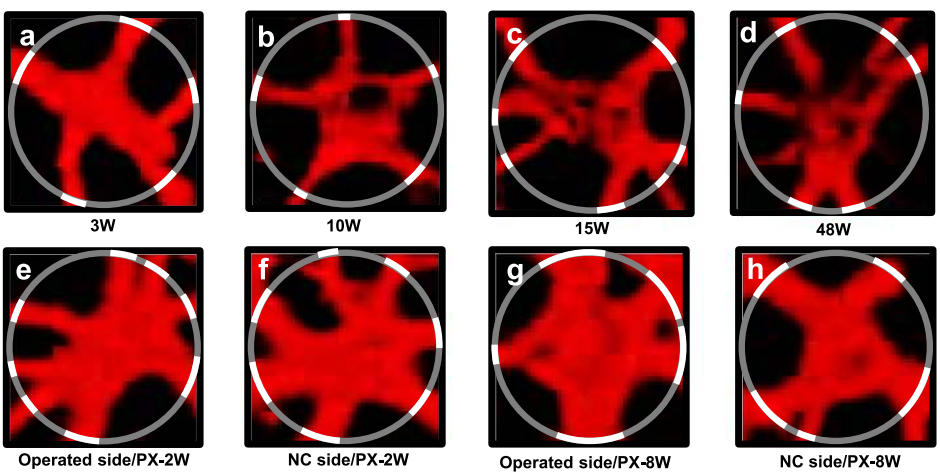

Fig. 10. Higher-magnified CLSM images of αSMA-immunostained myoepithelial cells of normal (**a–d**) and post-operative (**e–h**) submandibular glands of rats. White sections indicating the thickness of myoepithelial processes became longer in post-operated glands (**e–h**) than in normal glands (**a–d**).

at 48W (Fig. 8d). In the surgery groups, the number of primary processes (5.2–5.9) did not change in the operated and NC sides at PX-2W and PX-8W, whereas the number of terminal processes (33.7–40.3) significantly increased (Fig. 8e–h).

Thickness of processes

Processes became thicker on the operated and NC sides at PX-2W and PX-8W (Fig. 10e–h) than those in the normal group at 3, 10, 15, and 48W (Fig. 10a–d). The measurements of process thickness are shown in Figure 11. In the untreated normal submandibular gland, the mean thickness of 3, 10, 15, and 48W rats was 2.0–2.4 μm, showing no marked change. The mean thickness on the operated side of PX was 2.5 μm at PX-1W, showing no significant difference; however, the mean thickness from PX-2W to PX-8W was 2.8–3.7 μm, showing that processes were significantly thicker than those in the untreated group at the same age (10–16W). On the NC side of PX, the mean thickness was 2.3 μm at PX-1W, showing no significant difference, whereas the mean thickness after PX-2W was 3.1 μm, showing that processes were significantly thicker than those in the untreated group at the same age at most of the time points examined (Fig. 11).

IV. Discussion

Role of MECs

Previous studies by electron microscopic analyses demonstrated that myofilaments parallel to the acinar basal surface were present in the body and processes of MECs [6, 8, 36, 43, 49], and that the contractile proteins composing

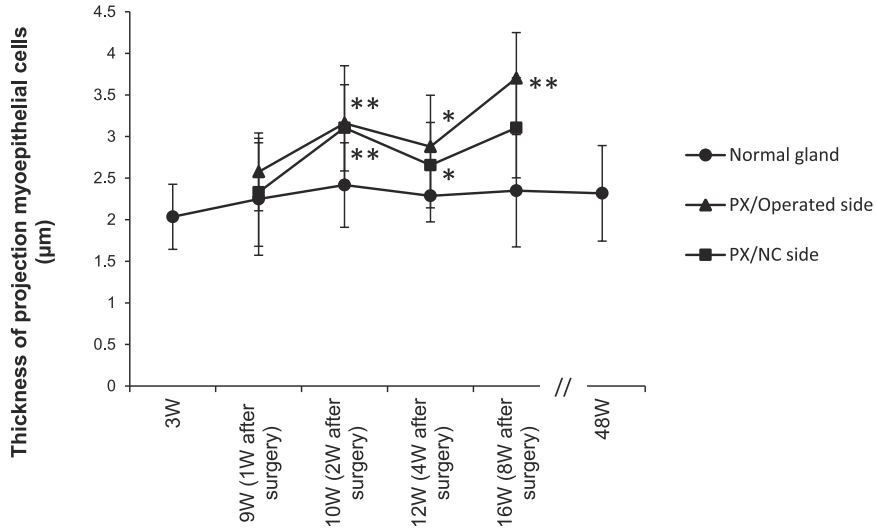

Fig. 11. Graph showing chronological changes in the thickness of myoepithelial processes. *: significant $p<0.05$. **: significant $p<0.01$.

the filaments, including actin and myosin, were common to those of smooth muscle cells [11, 36]. In addition, the enzyme activities observed in smooth muscle cells, such as alkaline phosphatase, ATPase, and glycogen phosphorylase, were also histochemically detected in MECs [36]. Based on these morphological and biochemical characteristics, MECs have been speculated to have contractile ability. Furthermore, since MECs and acinar cells adhere to each other through desmosomes, hemidesmosomes, and gap junctions, acini are considered to be compressed by the contraction of MEC processes [36, 43, 49]. The contraction of MECs in the salivary gland is induced predominantly by the parasympathetic nerve [36], isolated rat submandibular gland MECs were found to contract in response to an cholinergic or adrenergic stimulation [29], and acetylcholinesterase activity was absent in acinar cells, but present in MECs, suggesting that MECs possess a different parasympathetic regulatory system from that of acinar cells.

Regarding how MECs respond through changes in shape to a condition requiring a long-standing increase in secretion, previous studies showed that hypertrophy of MECs occurred in the mammary gland in response to pregnancy, and processes became complex, whereas acinar cells do not markedly change [32, 33, 47]. Our study found that the shape of MEC processes also markedly changed in the salivary gland, even though no change was noted in acinar or duct cells.

Relationship between the distribution and morphology of MECs and saliva secretion

Previous studies reported that MEC processes were thicker in the salivary gland secreting mucous saliva [6, 36]. Our results also clarified that the distribution and shape of MECs were associated with the properties of secreted saliva: MEC processes were thick, short, and simply ramified in the sublingual gland, which secretes mucous saliva [3, 16], whereas processes were thin, long, and complicated ramified in the submandibular gland, which secretes less mucous saliva [3, 16]. MECs were previously shown to be absent in the acini regions of the rodent serous parotid gland [3, 16]. The exocrine portion of the pancreas secreting pure serous pancreatic juice in humans and cats also lacks MECs [14], and we also did not find MECs in the normal 8W rat pancreas.

The mammary gland secretes relatively mucous milk, containing abundant amounts of fat in the lactation period, and MEC processes show a more complicated shape than that seen in a resting period [32, 33, 47]. The role of MECs in the salivary and mammary glands may become prominent and change the process shape as the viscosity of secretions increases.

Changes in the number and size of MECs

The number of MECs immunostained with αSMA increased on both the operated and NC sides after PX, and on the NC side after TX. Previous studies have shown that surgical treatments induce cell proliferation in the salivary gland [15, 40, 41]. The present results, therefore, suggest that surgical resection and incision of the unilateral submandibular gland induce proliferation of MECs in residual and NC glandular tissues.

The rate of the area occupied by MECs was higher in 3W normal than in normal rats at the other ages; however, acini were immature at 3W and contained cells derived from the fetal terminal tubules [1, 2, 30], and their size was smaller than that after 8W, which may have increased the number of acini present in the same area.

The area of the αSMA-positive region on immunostaining, used as an index of the MEC size, did not change at 8–16W in the untreated group, whereas it significantly increased after PX and TX. These increases in area after surgery were noted not only on the surgical, but also on the

NC side, thereby clarifying that the partial loss of salivary gland tissue by surgery induced MEC enlargement in the residual tissue within a short time, and this condition continued thereafter.

Changes in MEC processes

In 3W normal rats, more MECs were distributed in the intercalated duct than in acini, the number of terminal processes was smaller than that at 9W, and processes were also slightly narrower. Because bolus formation is unnecessary during the suckling period, the role of saliva may be smaller than after weaning. In the rat submandibular gland, acinar cells differentiate and grow from the fetal period to 5W, while MECs rapidly grow from birth to 2W or 3W old [8]. In addition, functional differentiation in contraction occurs in MECs after weaning [30], suggesting that the morphology and function of MECs in the submandibular gland were immature in 3W rats.

In normal 48W rats, the numbers of visible MEC bodies and processes and process thicknesses did not significantly increase from 9W, and only the area representing the MEC size significantly increased. In humans, saliva secretion decreases and saliva viscosity increases with aging [22]. Enlargement of MECs is suggested to occur in association with an increase in saliva viscosity induced by lower secretion.

Regarding the length of MEC processes, the frequency by which MEC processes crossed over the equator of acini and overlapped with the processes of MECs present at the opposite pole was greater in the experimental groups than in the untreated group. Extended processes finely surrounded the acinar surface, suggesting that they load a strong contractile force on the acinus.

Regarding the number of processes, Nagato [27] reported that the number of terminal processes of normal submandibular gland MECs was 20–30, which is consistent with that of the untreated submandibular gland in the present experiment. In contrast, this number was significantly higher after surgical treatment than that in the untreated group. The number of primary processes did not change in either the untreated or experimental group, demonstrating that the branching of MEC processes increased at a site distant from, and not close to the cell body.

The thickness of processes was 2.2–2.4 μm in the untreated group, which is consistent with that reported by Nagato [27]. Process thickness was greater after surgical treatment than in the untreated group, and did not return to the thickness level of the untreated group within the experimental period.

Our study clarified that surgical treatment of the unilateral submandibular gland induced increases in the length, number, and thickness of MEC processes on both the operated and NC sides, therefore, MEC morphology changed in a complicated manner. The acinar surface covered by MECs increased through these complicated morphological changes. The contraction of MEC processes assists in saliva secretion by loading pressure on acini [36]. Since salivary gland tissue was decreased by surgery, residual tissues are required to compensate for saliva secretion to maintain the secretory volume [18, 19]. Secretory function was enhanced in salivary glands after excision of the same and/or other salivary glands in rats [18, 19], and in humans [9].

Conclusion

The result of the present study strongly suggested that, in the rat salivary gland after surgery, the sophistication of MEC processes, an increase in length, number, thickness, and branching of processes, occurs to load a stronger contractile force on acini to promote saliva secretion.

V. Acknowledgments

This work was partially supported by JSPS KAKENHI Grant Number 26462796 to O.A.; and based on the doctoral thesis of Y. Kawabe submitted to the Graduate School of Dentistry, Meikai University.

VI. References

1. Amano, O. and Iseki, S. (1998) Occurrence and nuclear localization of cAMP response element-binding protein in the postnatal development of the rat submandibular gland. *Histochem. J.* 30; 591–601.
2. Amano, O., Kudo, Y., Shimada, M., Wakayama, T., Yamamoto, M. and Iseki, S. (2001) Transient occurrence of 27 kDa heat-shock protein in the terminal tubule cells during postnatal development of the rat submandibular gland. *Anat. Rec.* 264; 358–366.
3. Amano, O., Mizobe, K., Bando, Y. and Sakiyama, K. (2012) Anatomy and histology of rodent and human major salivary glands—Overview of the japan salivary gland society-sponsored workshop—. *Acta Histochem. Cytochem.* 45; 241–250.
4. Ban, T., Takizawa, N., Nagao, N. and Kusano, N. (1935) Über die beziehungen zwichen der inneren sekretion der speichel drüse und der entwicklung und dem wachstum des knochens (Der erste Bericht). *Proc. Jpn. Soc. Pathol.* 25; 510–511.
5. Bando, Y., Yamamoto, M., Sakiyama, K., Inoue, K., Takizawa, S., Owada, Y., Iseki, S., Kondo, H. and Amano, O. (2014) Expression of epidermal fatty acid binding protein (E-FABP) in septoclasts in the growth plate cartilage of mice. *J. Mol. Histol.* 45; 507–518.
6. Brocco, S. L. and Tamarin, A. (1979) The topography of rat submandibular gland parenchyma as observed with SEM. *Anat. Rec.* 194; 445–460.
7. Catalán, M. A., Nakamoto, T. and Melvin, J. E. (2009) The salivary gland fluid secretion mechanism. *J. Med. Invest.* 56; 192–196.
8. Chaudry, A. P., Schmutz, J. A., Cutler, L. S. and Sunderraj, M. (1983) Prenatal and postnatal histogenesis of myoppithelium in hamster submandibular gland. An ultrastructural study. *J. Submicrosc. Cytol.* 15; 787–798.
9. Chaushu, G., Dori, S., Sela, B. A., Taicher, S., Kronenberg, J. and Talmi, Y. P. (2001) Salivary flow dynamic after protid surgery: A preliminary report. *Otolaryngol. Head. Neck. Surg.* 124; 270–273.
10. Dardick, I., Rippstein, P., Skimming, L., Boivin, M., Parks, W. R. and Dairkee, S. H. (1987) Immunohistochemistry and

ultrastructure of myoepithelium of the ducts of human major slivary glands: Histogenetic implication for salivary gland tumor. *Oral Surg. Oral Med. Oral Pathol.* 64; 703–715.
11. Drenckhahn, U., Stewart, U. G. and Unsicker, K. (1977) Immunofluorescence-microscopic demonstration of myosin and actin in salivary glands and exocrine pancreas of the rat. *Cell Tissue Res.* 183; 273–279.
12. Emmelin, N. and Gjörstrup, P. (1973) On the function of myoepithelial cells in salivary gland. *J. Physiol.* 230; 185–198.
13. Fattah, E. A. A. (2008) Histological and immunohistochemical study of change in the slbino rat pancreas during aging. *Egypt J. Histol.* 31; 266–277.
14. Garrett, J. R., Lenninger, S. and Ohlin, P. (1970) Concerning possible contractile mechanism in the pancreas—Myoepithelial cells. *Experientia* 26; 741.
15. Hanks, C. T. and Chaudhry, A. P. (1971) Regeneration of rat submandibular gland following partial extirpation. A light and electron maicroscopic study. *Am. J. Anat.* 130; 195–208.
16. Jenkins, G. N. (1978) Saliva. In "The Physiology and Biochemistry of the Mouth. vol. 4", Blackwell Scientific Publication, Victoria, pp. 284–359.
17. Kawaguchi, M. and Yamagishi, H. (1995) Receptive system for drugs in salivary gland cells. *Folia Pharmacol. Jpn.* 105; 295–303.
18. Kawai, T. (1957) Experimental study on the relationship between secretory function of the submandibular gland cells and increased histamine in the blood after the perfect extripation of the parotid glands. *Arch. Hist. Jpn.* 13; 391–400.
19. Kawai, T. (1958) Studies on the effects of the extripation of the submandibular and sublingual glands on the secretory function of the parotid gland cells and on histamine in the blood. *Arch. Hist. Jpn.* 14; 397–408.
20. Kierszenbaum, A. L. (2007) Digestive glands. In "Histology and Cell Biology. 2nd ed.", Elsevier, PA, pp. 485–513.
21. Laine, M. and Virtanen, R. L. (1996) Effect of hormone replacement therapy on salivary flow rate, Buffer effect and pH in perimenopausal and postmenopausal women. *Arch. Oral Biol.* 41; 91–96.
22. Mashita, J., Okane, M., Satoh, Y., Kitagawa, N. and Kitamura, Y. (2008) Relationship between oral dryness and properties of saliva (I): Healthy adults. *J. J. Gerodont.* 23; 319–329.
23. Matsuo, R. (2006) Central nervous system for salivary secretion. *Folia Pharmacol. Jpn.* 127; 261–266.
24. Miyashita, T., Okubo, M., Shinomiya, T., Nakagawa, K. and Kawaguchi, M. (2011) Pregnenolone biosynthesis in the rat salivary gland and its inhibitory effect on secretion. *J. Pharmacol. Sci.* 115; 56–62.
25. Mizobe, K., Kawabe, Y., Bando, Y., Sakiyama, K., Araki, H. and Amano, O. (2014) Localization of Hsp27 in the rat submandibular gland following the application of various surgical treatment. *Acta Histochem. Cytochem.* 47; 255–264.
26. Morinaga, S., Nakajima, T. and Shimosato, Y. (1987) Normal and neoplastic myoepithelial cells in salivary glands. *Hum. Pathol.* 18; 1218–1226.
27. Nagato, T. (1980) Scanning and transmission electron microscope study of myoepithelial cells in some exocrine glands of the rat. *J. Kyushu. Dent. Soc.* 34; 103–118.
28. Nazeer, J., Prakash, V., Mandal, S. and Prakash, A. (2014) Myoepithelal cells: Structure, function and role in tumor formation. *Int. J. Dent. Health. Sci.* 1; 155–160.
29. Nishikawa, A., Katoh, K., Saitoh, S. and Wakui, M. (1980) Effect of neural stimulation on contractile system (myoepithelial cells) in isolated salivary gland segments of rat. *Membr. Biochem.* 3; 317–328.
30. Ogawa, Y., Yamauchi, S., Ohnishi, A., Ito, R. and Ijuhin, N. (1999) Immunohistochemistry of myoepithelial cells during development of the rat salivary glands. *Anat. Embryol. (Berl.)* 200; 215–228.
31. Proctor, G. B. and Carpenter, G. H. (2014) Salivary secretion: mechanism and neural regulation. *Monogr. Oral Sci.* 24; 14–29.
32. Radnor, C. J. (1972) Myoepithelium in the prelactating and lactating mammary glands of the rat. *J. Anat.* 112; 337–353.
33. Radnor, C. J. (1972) Myoepithelium in involuting mammary glands of the rat. *J. Anat.* 112; 355–365.
34. Rafael, M. and Dolores, G. (2004) Unilateral agenesis of the parotid gland: A case report. *Oral Surg. Oral Med. Oral Pathol. Oral Radiol. Endod.* 98; 712–714.
35. Raubenheimer, E. J. (1987) The myoepithelial cell: Embryology, function, and proliferative aspects. *Crit. Rev. Clin. Lab. Sci.* 25; 161–193.
36. Redman, R. S. (1994) Myoepithelium of salivary glands. *Microsc. Res. Tech.* 27; 25–45.
37. Scully, C. (2003) Drug effects on salivary glands: dry mouth. *Oral Dis.* 9; 165–176.
38. Sheetz, J. H., Morgan, A. H. and Schneyer, C. A. (1983) Morphological end biochemical in the rat parotid gland after compensatory and isoprotenol-induced enlargement. *Arch. Oral Biol.* 28; 441–445.
39. Sugiya, H. (2011) Mechanism of salivary secretion. *Jpn. J. Oral Maxillofac. Surg.* 57; 182–186.
40. Takahashi, S., Nakamura, S., Suzuki, R., Domon, T., Yamamoto, T. and Wakita, M. (1999) Changing myoepithelial cell distribution during regeneration of rat parotid glands. *Int. J. Exp. Pathol.* 80; 283–290.
41. Takahashi, S., Kohgo, T., Arambawatta, A. K. S., Domon, T. and Wakita, M. (2005) Biological behavior of myoepithelial cells in the regeneration of rat atrophied sublingual glands following release from duct ligation. *J. Mol. Histol.* 36; 373–379.
42. Takizawa, N., Nagao, N., Kusano, N. and Hayami, H. (1936) Über die beziehungen zwichen der inneren sekretion der speichel drüse und der entwicklung und dem wachstum des knochens (Der zweiter Bericht). *Proc. Jpn. Soc. Pathol.* 26; 529–530.
43. Tamarin, A. (1966) Myoepithelium of the rat submaxillary gland. *J. Ultrastruct. Res.* 16; 320–338.
44. Tomas, F. M. (1974) The influence of parathyroid hormone on the secretion of phosphate by the parotid salivary gland of sheep. *Q. J. Exp. Physiol.* 59; 269–281.
45. Utsunomiya, Y., Sawaki, K., Kawaguchi, M. and Yamaguchi, H. (2007) Sex hormones and functional modification of salivary gland. *Shikwa Gakuho.* 107; 163–169.
46. Vinayak, V., Annigeri, R. G., Patel, H. A. and Mittal, S. (2013) Adverse affects of drugs on saliva and salivary glands. *J. Orofac. Sci.* 5; 15–20.
47. Yamazaki, Y. (1977) Ultrastructural study of rat mammary glands under hormonal influences. *J. O. M. A.* 89; 1359–1380.
48. Yoshitomi, A., Kuwata, H., Suzuki, T., Masuda, M., Narishima, M., Nakajima, T., Imokawa, S., Suda, T., Ghida, K. and Nakamura, H. (2000) Compensatory growth of residual lung after pneumonectomy in childhood. *A. J. R. S.* 38; 642–644.
49. Young, J. A. and Van, L. E. W. (1977) Morphology and physiology of salivary myoepithelial cells. *Int. Rev. Physiol.* 12; 105–125.